FARADAY

Oxyhalogen–sulfur chemistry

Oxidation of 2-aminoethanethiolsulfuric acid by iodate in acidic medium†

Claudius Mundoma and Reuben H. Simoyi*

Department of Chemistry, West Virginia University, P.O. Box 6045, Morgantown, WV 26506-6045, USA

The oxidation of 2-aminoethanethiolsulfuric acid, AETSA, by iodate has been studied in highly acidic media. The reaction is very slow and shows some clock-reaction characteristics in which iodine is formed after some induction period. The oxidation of AETSA involves the oxidation of only one of the sulfur atoms to SO_4^{2-}. The other sulfur atom remains attached to the carbon chain as a sulfonic acid (taurine). The stoichiometry of the reaction is: $IO_3^- + H_2NCH_2CH_2S{-}SO_3H + H_2O \rightarrow H_2NCH_2CH_2SO_3H + I^- + SO_4^{2-} + 2H^+$. The reaction of I_2 and AETSA was found to be slow and autoinhibitory as the I^- formed combines with the remaining I_2 to form the relatively unreactive triiodide ion, I_3^-. The second-order rate constant for the reaction between I_2 and AETSA was determined as 16.7 ± 2.3 M^{-1} s^{-1}.

Recently, we embarked on a systematic study of the kinetics and mechanisms of several reactions which involve sulfur compounds.[2] The recurring theme in oxidation reactions of sulfur compounds has been the omnipresent complexities in global reaction dynamics.[3] A generalized algorithm for a generic pathway of sulfur compound oxidations has not been formulated, despite the numerous kinetic studies performed so far. There are several possible ways of obtaining exotic dynamics with sulfur-containing compounds such that nearly each system studied has its own peculiarities.[4]

Though oxyhalogens and sulfur compounds are very important species in environmental studies; there exists scant knowledge on how they react. Sulfur chemistry is very complex and is subject to stochastic behaviour which is fueled by free radical mechanisms.[5,6] Sulfur chemistry is also extremely sensitive to the pH of the environment,[7,8] which explains the inherent difficulties encountered in environmental sulfur abatement procedures.[9]

Prior to the discovery of sulfur chemistry as a source of exotic reaction dynamics oxyhalogen chemistry had been the major source of non-linear dynamics in chemistry.[10,11] The most well known exotic dynamics is oscillatory behaviour. Nearly all previously known aqueous solution chemical oscillators which were accidentally discovered involved oxyhalogen chemistry.[12–16] It has been easier, over the years, to deduce a generalized reaction scheme on how oxyhalogens produce non-linear behaviour.[17] It is now established that oxyhalogens rely on complex feedback mechanisms such as autocatalysis and/or autoinhibition to generate non-linear behaviour.[18]

One, seemingly omnipresent, characteristic in sulfur chemistry is the propensity to form S—S bonds and to polymerise.[19] In large enough and sterically hindered organic sulfur compounds dimer formation is routinely observed.[20] Dimer formation or any other form of aggregation represent an in-built mechanism for the generation of non-linear reaction dynamics, especially if the aggregates react at different rates compared to the monomer.

Here, we report on a kinetic and mechanistic study of the oxidation of 2-aminoethanethiolsulfuric acid, $H_2NCH_2CH_2S{-}SO_3H$, [AETSA] (which already contains an S—S bond), by iodate in acidic medium. We wanted to answer three relevant questions with respect to the reaction mechanism and hopefully use the same information on similar systems: (a) under what conditions does the S—S bond cleave? (b) Is it possible, with a mild to strong oxidizing agent such as IO_3^-, to be able to cleave the C—S bond and what products ensue? (c) What will be the role of the Dushman reaction[21] in the overall reaction dynamics once the oxidation has got underway?

† Part 18 in the series: Non-linear dynamics in chemistry derived from sulfur chemistry. Part 17: ref. 1.

Experimental

Reagents

Singly distilled water was used for the preparation of all stock solutions and for all purposes. Reagent grade potassium iodate (Aldrich) was used as supplied. Potassium iodate is a primary standard and its solutions are very stable under normal conditions. AETSA (Pfaltz and Bauer) was used without any further treatment, as was potassium iodide (Fisher). AETSA solutions were protected from light by covering the volumetric flasks with aluminium foil and storing them in the fridge when not in use. AETSA solutions exposed to light gave irreproducible kinetics results. Solutions were kept for a period of not more than 10 h, after which a new set of solutions was prepared to ensure reproducibility. Reagent grade sodium perchlorate and perchloric acid, 69–72% (Fisher) were used for ionic strength and pH adjustment, respectively. Iodine (Aldrich) solutions were prepared by dissolving the crystalline, resublimed 99.8% reagent grade solid in distilled water and allowing to stand overnight before using.

Methods

All experiments were performed at 25 ± 0.2 °C and reactions involving iodate were run under high acid concentration to give reasonable reaction rates. Reactions were run at an ionic strength of 1.0 M ($NaClO_4$). All photosensitive reagents were not only covered in aluminium foil but the room was also darkened to ensure minimal effect of the light. Iodine solutions were standardized by titrating against thiosulfate with freshly prepared starch as the indicator. The concentrations were also determined by measuring the absorbance at 465 nm where the molar absorption coefficient (ε) had been determined[22] as 771 M^{-1} cm^{-1}. The reaction progress was also followed by monitoring the organic substrate on a JEOL 270 MHz NMR spectrometer. Solutions for ^{1}H NMR studies were prepared using deuteriated solvents.

The reactions were slow enough to be run on the conventional Perkin-Elmer Lambda 2S UV–VIS spectrophotometer. Data were analysed for induction periods, maximum absorbance and initial rates on a 486-33 MHZ DEC computer.

Stoichiometric determinations

Stoichiometry of the iodate–AETSA reaction was determined by varying the amount of iodate whilst keeping the amounts of AETSA and acid constant. The solutions of varying ratios of iodate to AETSA were incubated for a 24 h period in a cool dark place and absorbance of the solutions were measured at 465 nm. The I_2 obtained was used to estimate the amount of excess iodate in solution. Sulfate was analysed gravimetrically as $BaSO_4$ using $BaCl_2$ as the precipitating reagent.[23] Excess iodate was also determined iodometrically using acidified excess iodide and subsequent thiosulfate titration.[24]

Iodine–AETSA reaction

Solutions used for stoichiometric determinations were also stored for at least a 24 h incubation period. Solutions were analysed quantitatively for unreacted iodine and for sulfate.

Results

Stoichiometry

The stoichiometry of the iodate–AETSA reaction was determined as:

$$IO_3^- + H_2NCH_2CH_2SSO_3H + H_2O \rightarrow H_2NCH_2CH_2SO_3H + SO_4^{2-} + 2H^+ + I^- \quad (1)$$

Stoichiometry (1) was valid only in high acid conditions. In excess IO_3^- conditions, $R = [IO_3^-]_0/[AETSA]_0 > 1$, the Dushman reaction[21] forms I_2 from the excess IO_3^- and the I^- formed from reaction (1):

$$IO_3^- + 5I^- + 5H^+ \rightarrow 3I_2(aq) + 3H_2O \quad (2)$$

Reaction solutions were mixed with varying $[IO_3^-]_0$ at fixed $[AETSA]_0$. Stoichiometry (1) was deduced as the highest $[IO_3^-]_0/[AETSA]_0$ ratio possible before I_2 is formed as one of the products after prolonged standing. The complexity in determining the stoichiometry arose from the fact that I_2, when it is formed, is a very poor oxidizer of AETSA. Thus initial accumulation of I_2 was not indicative of complete consumption of AETSA, and neither did it indicate that stoichiometry (1) had already been attained. The $[IO_3^-]$–[AETSA] system can be compared to the classic Landolt clock reaction[24] in which the oxidation of the reductant, HSO_3^-, by iodine is fast while the Dushman reaction is rate determining. The Landolt reaction thus shows a small iodine concentration spike as opposed to the slow monotonic iodine formation observed in this system. Excess of $[IO_3^-]$ ensured that, even though some of the IO_3^- was being converted to I_2, reaction (2), there still remained enough IO_3^- to continue the oxidation of AETSA. The excess oxidizing power ($IO_3^- + I_2$) was then determined *via* an iodometric titration.[25] In the limit of prolonged standing (up to 7 days), the stoichiometry of the reaction in excess IO_3^- is

$$6IO_3^- + 5H_2NCH_2CH_2SSO_3H + 2H_2O \rightarrow 5H_2NCH_2CH_2SO_3H + 5SO_4^{2-} + 4H^+ + 3I_2 \quad (3)$$

Stoichiometry (3) is a linear combination of stoichiometries (1) and (2): 5(1) + (2). Iodine was determined spectrophotometrically at $\lambda = 465$ nm as no other species in solution appeared to absorb at this wavelength. The sulfate analysis showed that only one of the S atoms was released as SO_4^{2-} and the other remained attached to the parent organic molecule to form the sulfur amino acid, taurine.[26,27] Taurine was detected by NMR spectroscopy. AETSA shows a single complex multiplet centred around δ 3.3. The multiplet is from the complex coupling between the adjacent methylene protons. The protons on the amino functionality are not observed owing to their rapid exchange with the solvent. Taurine shows distinct triplets whose position is influenced by the pH of the solution. In high acid strengths, the two peaks are shifted downfield. NMR spectra of the reaction solution were taken at regular intervals of *ca.* 1 min. The AETSA multiplet peak initially splits into two separate multiplets which finally resolve themselves into the standard taurine triplet pair. The iodine formed in stoichiometry (3) did not react with taurine. Mixtures of iodine and taurine showed no decrease in the iodine titre at the timescale of our experimental observations.

A separate stoichiometric determination was made for the I_2–AETSA reaction. This reaction is very slow, and stoichiometric determinations were performed after an incubation period of over 7 days. Even after 7 days, the stoichiometry was still inconclusive. Gravimetric analysis showed a faint and non-quantitative formation of sulfate. ^1H NMR data shows that the product contains a mixture of taurine, the sulfoxide, $H_2NCH_2CH_2S(O)SO_3H$, and the sulfone, $H_2NCH_2CH_2S(O_2)SO_3H$. The sulfoxide was the easiest to detect by ^1H NMR technique. After 1 day of incubation, it appeared the stoichiometry of the reaction was

$$I_2(aq) + H_2NCH_2CH_2SSO_3H + H_2O \rightarrow 2I^- + H_2NCH_2CH_2S(O)SO_3H + 2H^+ \quad (4)$$

The chiral sulfur centre renders the two α-protons diastereotopic. Thus they split the β-protons into two separate doublets with the α-protons showing up as two separate multiplets, integrating as a single proton each and separated by *ca.* 1.5 ppm. The chemical environments around the α-protons are so different that they each independently couple with the equivalent β-protons to give a triplet which is further coupled to the other diastereotopic proton to give a complex multiplet.

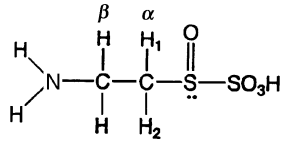

Further incubation of the reaction solution and subsequent oxidation of the sulfoxide to the sulfone destroyed this pattern. If I_2, however, is first titrated with NaOH, the end

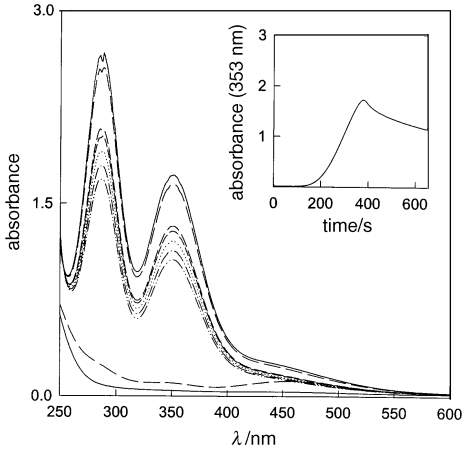

Fig. 1 Spectral scans between $\lambda = 250$ and 600 nm in conditions of excess AETSA. Initially the peaks at 286, 353 and 470 nm all increase as I_2 and I_3^- are formed. Later all these peaks disappear as I_2 and I_3^- are consumed by the excess AETSA. The insert shows the absorbance–time trace for these scans at the 353 nm peak. $[IO_3^-]_0 = 0.001$ M; $[H^+]_0 = 0.400$ M; $[AETSA]_0 = 0.003$ M.

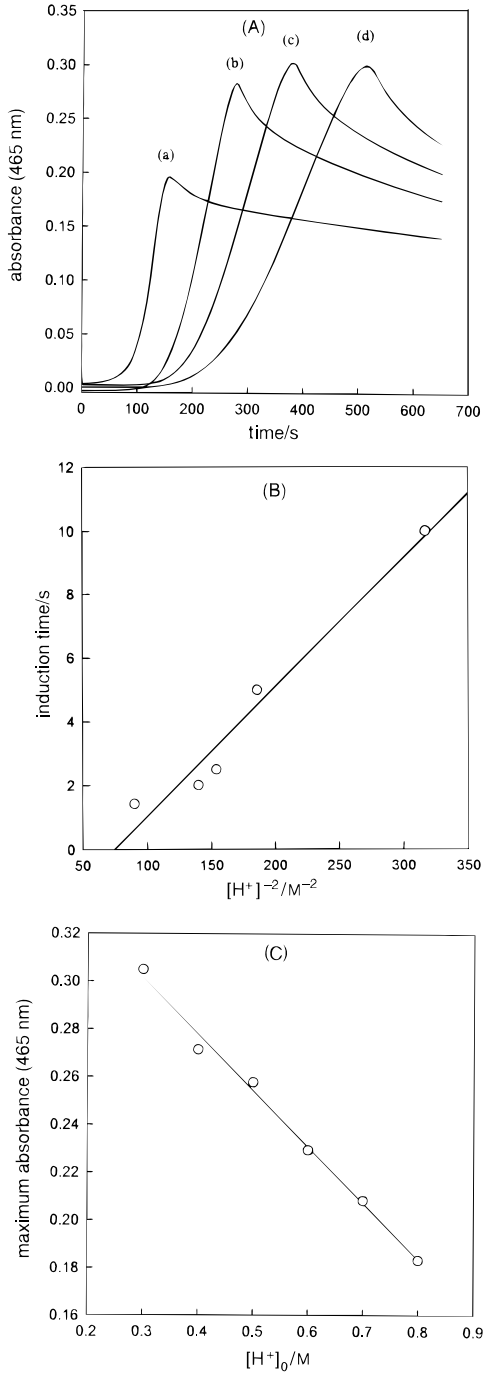

Fig. 2 A, Absorbance traces at $\lambda = 465$ nm in excess AETSA over IO_3^-. Total consumption of I_2 can take up to 24 h. $[IO_3^-]_0 = 0.001$ M; $[AETSA]_0 = 0.005$ M. $[H^+]_0$: (a) 0.800; (b) 0.400; (c) 0.200; (d) 0.100 M. B, Induction time *vs.* the square of the inverse of the initial acid concentrations $[IO_3^-]_0 = 0.001$ M; $[AETSA]_0 = 0.005$ M. C, Dependence of maximum transient I_2 obtained with respect to initial acid concentrations. Initial conditions as in B.

point being the point where the brown iodine colour disappears or the point where the pH rapidly changes to basic, the solution so obtained did produce sulfate with AETSA after at least a 3 day incubation period. While molecular iodine could not quantitatively cleave the S—S bond, it appears as if hypoiodous acid, HOI, can.

Reaction dynamics

The reaction presented some very complex reaction patterns although it had a featureless spectrum with peaks at 286, 353 and 470 nm only (Fig. 1). These three peaks grew with time in the IO_3^-–AETSA reaction and they decayed in the

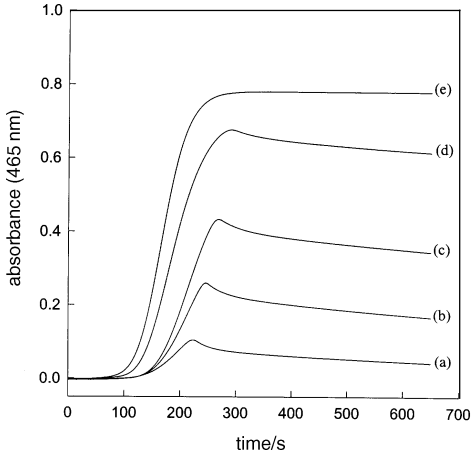

Fig. 3 Absorbance traces at 465 nm with varying $[IO_3^-]_0$. Final I_2 absorbance for all 5 traces is zero, but after reaction times of up to 168 h. $[H^+]_0 = 0.500$ M; $[AETSA]_0 = 0.005$ M. $[IO_3^-]_0$: (a) 0.005; (b) 0.001; (c) 0.0015; (d) 0.002; (e) 0.004 M.

I_2–AETSA reaction. The peaks at 286 and 353 nm were due to the I_3^- species, while the peak at 470 nm is due to the aqueous I_2 species. The reaction could be followed at any of these three peaks. A time trace at $\lambda = 353$ nm of the spectral scan data is shown on the insert of Fig. 1. The trace at $\lambda = 470$ nm had the same shape as the one at $\lambda = 353$ nm but with much lower absorbance readings as can be observed in the scans shown in Fig. 1. Spectrophotometric determinations were carried out at 465 nm which was the experimentally determined isosbestic point for I_2 and I_3^- species.

Depending upon initial conditions, the reaction ($\lambda = 465$ nm) started with an induction period in which no activity is observed in the absorbance or redox potential traces. At the end of the induction period, I_2 is formed. With $R = [IO_3^-]_0/[AETSA]_0 > 5$ there was a monotonic increase in the I_2 formation over the entire range of acid concentration used until a saturation value is reached. With $R \leqslant 2$, the I_2 concentration increases to a peak value and then is slowly consumed (Fig. 2A) to reach some final value which is determined by stoichiometry (3), or with $R < 1$, the iodine concentration will vanish to zero [stoichiometry (1)]. Three reaction parameters were derived from the absorbance traces: (a) the length of the induction period; (b) the maximum absorbance observed at $\lambda = 465$ nm; (c) the rate of consumption of I_2 after attaining the peak concentration.

Acid dependence. The most important parameter in determining the reaction dynamics and rate of reaction was the acid concentration. The reaction system showed no noticeable activity when the acid concentrations were lower than 0.10 M. Acid affects the length of the induction period to the inverse square power (Fig. 2A and B). A log–log plot of induction period *vs.* $[H^+]_0^{-1}$ gave a slope 2.1 ± 0.2. This shows that the precursor reaction for the formation of I_2 is accelerated by acid to the second power. One rather surprising fact was that the maximum amount of transient I_2 formed decreased linearly with $[H^+]_0$ (Fig. 2C). Traces with the longer induction times (low acid) gave much slower rates of formation of I_2. High acid concentrations had shorter induction times and much faster formation rates for I_2. Stoichiometry is thus quickly attained with high acid concentrations.

Iodate dependence. Iodate concentrations can determine if a monotonic I_2 formation occurs (Fig. 3). For low R values, the iodine concentrations attain a peak value before subsequently decaying to zero. At higher $[IO_3^-]_0$, I_2 is formed until it reaches its final stoichiometric equivalent concentration [stoichiometry (3)]. There is an inverse relationship between

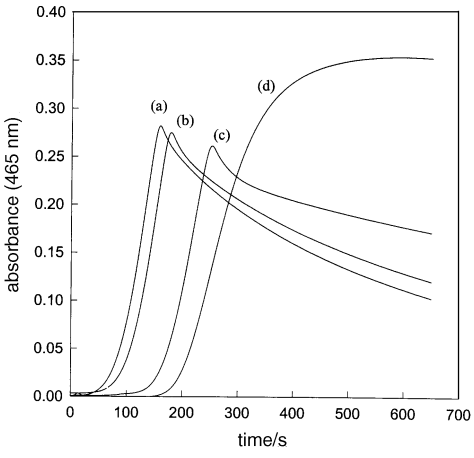

Fig. 4 Traces with excess AETSA (a)–(c) show transient I_2 formation while trace (d), with excess IO_3^-, shows a monotonic increase in I_2. $[IO_3^-]_0 = 0.001$ M; $[H^+]_0 = 0.500$ M. $[AETSA]_0$: (a) 0.020; (b) 0.015; (c) 0.005; (d) 0.0002 M.

induction time and the initial iodate concentrations. With low IO_3^- concentrations and stoichiometric excess of AETSA; stoichiometry (1) will prevail as the I^- formed from the reaction will not have sufficient IO_3^- available to enable formation of I_2. Traces in Fig. 3(a)–(c) show that any of the I_2 formed through reaction (2) will be consumed by the excess AETSA while Fig. 3(d) and (e), with higher $[IO_3^-]_0$, show sustained formation of I_2. The maximum (transient) I_2 formed

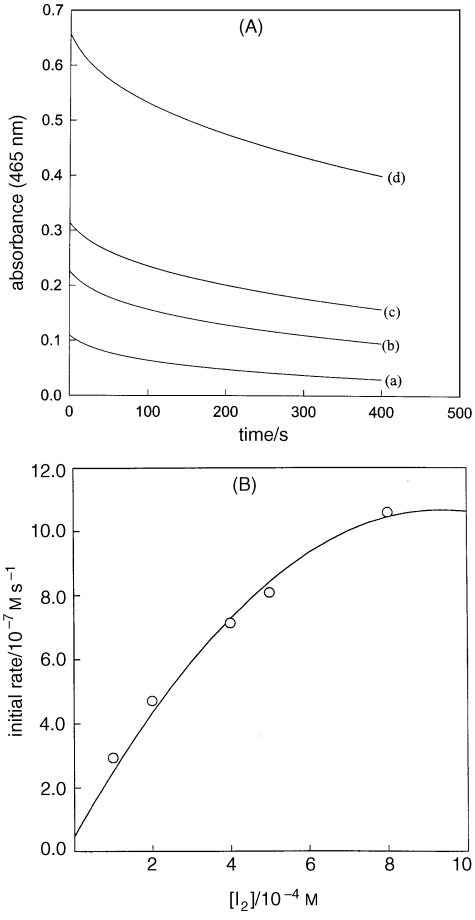

Fig. 5 A, Absorbance traces at 465 nm for the I_2–AETSA reaction. Reaction quickly slows down due to product inhibition. $[AETSA]_0 = 0.020$ M. $[I_2]_0$: (a) 0.0002; (b) 0.0004; (c) 0.0005; (d) 0.0008 M. B, Variation of the initial rate of the I_2–AETSA reaction with respect to $[I_2]_0$. The saturation curve is typical of autoinhibitory reactions. $[AETSA]_0 = 0.020$ M.

is proportional to $[IO_3^-]_0$. This has been obtained despite the competing reactions (formation of I_2 and its consumption *via* reduction by AETSA).

AETSA dependence. The type of reaction dynamics obtained from $[AETSA]_0$ variation is very similar to that obtained from $[IO_3^-]_0$ variations as the same value of R controlled both concentrations. Fig. 4 shows a series of experiments run at different $[AETSA]_0$ for fixed $[IO_3^-]_0$ and $[H^+]_0$. With very low $[AETSA]_0$, $R > 5$, one observes the normal induction period followed by saturation [Fig. 4(d)]. Higher $[AETSA]_0$ encourage rapid I_2 formation followed by an equally rapid consumption [Fig. 4(a)–(c)]. The induction period was found to decrease with increase in $[AETSA]_0$ as has been observed in the Landolt reaction[24] where the induction period is inversely proportional to the concentrations of both the oxidant and reductant. Other systems we had studied had given induction periods which were inversely proportional to the initial concentrations of the reductant and directly proportional to the concentrations of the oxidant.[28] A decrease in induction period is possible if (a) consumption of I_2, once formed, is very slow [reaction (4) slow]; (b) Dushman reaction, (2), is much faster than either reaction (1) or (4); (c) I^- acts as an autocatalyst in the reaction system or (d) a combination of all three.

Iodine–AETSA reaction

The I_2–AETSA reaction is so important in this mechanism that a separate kinetics study was initiated. The reaction is quite slow, and it quickly slows down even further as the reaction progresses into what appears to be autoinhibition. Fig. 5A shows the absorbance traces at 465 nm with varying initial iodine concentrations. A plot of initial rate *vs.* $[I_2]_0$ shows a saturation curve (Fig. 5B).

The first product which results from I_2 reduction which was investigated was I^-. Fig. 6A shows the strong inhibitory effect of I^- on the reaction. The reaction effectively shuts down when $[I^-]_0 \geqslant [I_2]_0$ [Fig. 6A(d)]. The relationship between $[I^-]_0$ and initial rate is shown in Fig. 6B. An inverse plot (initial rate)$^{-1}$ *vs.* $[I^-]_0$ gave a straight line.

The effect of acid on the reaction was also inhibitory (Fig. 7A and B). The acid inhibition was not as severe as that of I^-. The initial rate also showed an inverse dependence on the initial iodide concentrations (Fig. 7B).

Mechanism

The data from the induction periods (*e.g.* Fig. 2B) suggest that the standard initiation reaction for the Dushman reaction[21] is the rate-determining step in this reaction system:

$$IO_3^- + I^- + 2H^+ \rightleftharpoons HIO_2 + HOI \quad (5)$$

With reaction (5) rate-determining the squared acid dependence term and the first power IO_3^- dependence can easily be justified.

Only trace amounts of I^- are needed for reaction (5) because any I^- used will be generated by further reduction of the oxyiodine species generated in the reaction:

$$HOI + H_2NCH_2CH_2S{-}SO_3H \rightarrow H_2NCH_2CH_2S(O)SO_3H + I^- + H^+ \quad (6)$$

where $H_2NCH_2CH_2S(O)SO_3H$ is the sulfoxide of AETSA. Combination of reactions (5) and (6) gives the composite reaction which represents direct IO_3^- attack on AETSA:

$$IO_3^- + H_2NCH_2CH_2S{-}SO_3H + H^+ \rightarrow H_2NCH_2CH_2S(O)SO_3H + HIO_2 \quad (7)$$

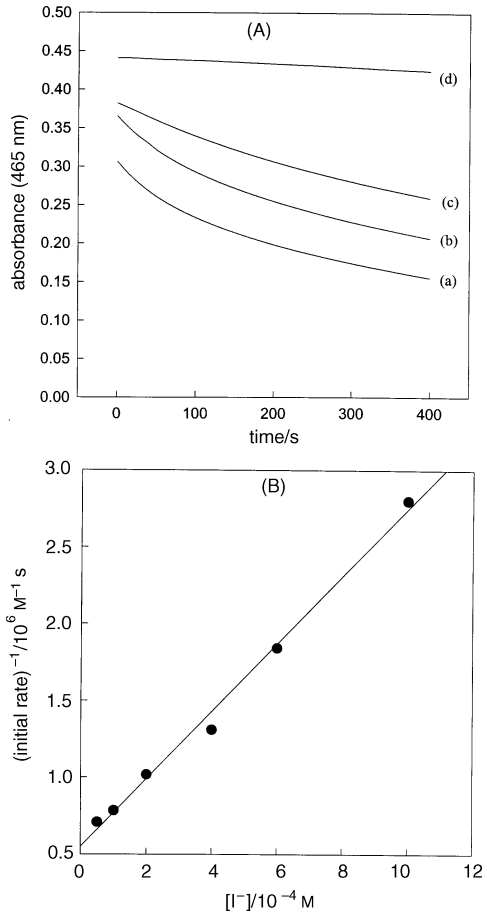

Fig. 6 A, Absorbance traces showing the inhibitory effect of I^- on the I_2–AETSA reaction. $[I_2]_0 = 0.0005$ M; $[AETSA]_0 = 0.005$ M. $[I^-]_0$: (a) 0.00005; (b) 0.0001; (c) 0.0004; (d) 0.003 M. B, Inverse of initial rate *vs.* $[I^-]_0$ for the data in Fig. 6A showing the linear dependence.

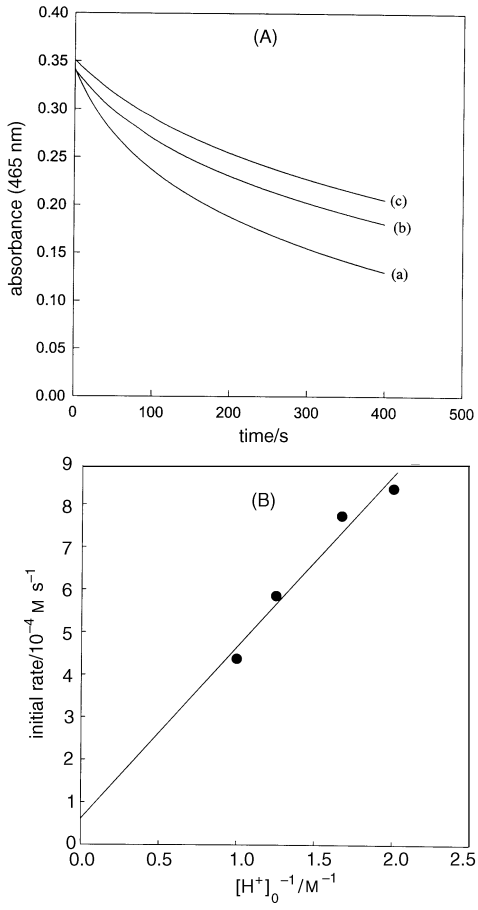

Fig. 7 A, Inhibitory effect of $[H^+]_0$ on the I_2–AETSA reaction. $[I_2]_0 = 0.0005$ M; $[AETSA]_0 = 0.005$ M. $[H^+]_0$: (a) 0.10; (b) 0.40; (c) 0.60 M. B, Acid dependence of the initial rate of the acid concentrations. Initial conditions are the same as in A.

With reaction (5) being rate determining, the rate of reaction becomes:

$$-d[IO_3^-]/dt = k_5[IO_3^-][I^-][H^+]^2 - k_{m5}[HIO_2][HOI] \quad (I)$$

where k_{m5} is the reverse rate constant for reaction (5). Since $[IO_3^-]_0$, $[H^+]_0 \gg [I^-]_0$, $[HIO_2]_0$ and $[HOI]_0$, then the reverse reaction will be negligible and the reaction will proceed quantitatively to the right. The squared acid dependence term eliminates reaction (7) as a possible elementary rate-determining step.

Oxidation of AETSA is primarily through hypoiodous acid, HOI. Iodous acid, HIO_2, readily reacts with I^- to produce HOI:[29]

$$HIO_2 + I^- + H^+ \rightleftharpoons 2HOI \quad (8)$$

HOI can then oxidize AETSA [reaction (6)] or react with I^- to form I_2:[30]

$$HOI + I^- + H^+ \rightleftharpoons I_2(aq) + H_2O \quad (9)$$

Iodine concurrently oxidizes AETSA, albeit slowly, reaction (4). I^- is the control reagent which produces the reactive oxyiodine species from IO_3^-. Fig. 8 shows a series of absorbance traces generated by the additions of small amounts of I^-. Iodide, (a) decreases the induction period, (b) increases the amount of transient I_2 formed and (c) decreases the rate of consumption of the transient I_2 once it is formed. The effect of I^- on the IO_3^-–AETSA reaction is inhibitory, despite the decreased induction period.

Introduction of I^- in an environment with I_2(aq) produces a relatively unreactive electrophile, I_3^-:[31]

$$I_2(aq) + I^- \rightleftharpoons I_3^-(aq) \quad (10)$$

I_3^- will react only very slowly with AETSA as in reaction (11).

$$I_3^- + AETSA + H_2O \rightarrow H_2NCH_2CH_2S(O)SO_3H + 3I^- + 2H^+ \quad (11)$$

Decrease in induction period with I^- (Fig. 8) indicates that reactions (8) and (9) are enhanced and rapidly form I_2

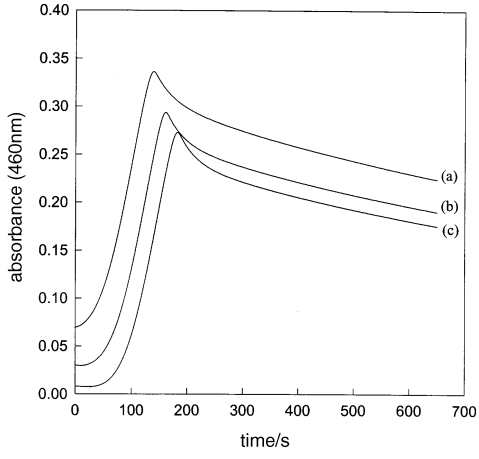

Fig. 8 Effect of I^- on the IO_3^-–AETSA reaction. $[H^+]_0 = 0.400$ M; $[AETSA]_0 = 0.0056$ M; $[I_2]_0 = 0.0005$ M. $[I^-]_0$: (a) 2.0×10^{-4}; (b) 8×10^{-5}; (c) 2.0×10^{-5} M.

although this does not indicate the status of the oxidation of AETSA. Addition of I^- enhances reactions (5), (8) and (9) but inhibits the oxyiodine–AETSA reactions, especially reaction (4).

HOI can form further reactive species from IO_3^- much more rapidly than I^-:[32]

$$IO_3^- + HOI + H^+ \rightleftharpoons 2HIO_2 \qquad (12)$$

Reaction (12) controls the concentration of HOI in reactions involving IO_3^- as the oxidant. I^- in solution will consume HOI *via* reaction (9). Reaction (9) was studied by Eigen and Kustin[30] who found it to be very rapid (almost diffusion controlled) in the direction in which it is written.

Acid dependence

With $R < 1$, low acid concentrations give long induction periods and higher transient I_2 concentrations (Fig. 2A). High acid concentrations enhance reaction (5). What is, however, the effect of acid on reactions (4) and (6)? With reaction (5) being the sole rate-determining reaction, the inverse squared dependence of the induction period can be rationalized from eqn. (I). Acid, however, inhibits the consumption of I_2, *i.e.* reactions (4) and (11). Since acid effects on the formation and the consumption of I_2 are opposite, the observed overall effect will depend on which effect is stronger. The observed decrease in $[I_2]_{max}$ with acid shown in Fig. 2A is only relevant when the final iodine concentration is zero; *i.e.* stoichiometry (1) environments. Acid not only catalyses the I_2 formation, but also the oxyiodine–AETSA reactions. Thus less of the intermediate, I_2, is formed at high acid concentrations.

Acid retardation of the I_2–AETSA reaction can have two plausible mechanisms or a combination of both: (a) if reaction (6) is faster than reaction (4), then acid would retard the rate of AETSA oxidation through the equilibrium of reaction (9). The rate of I_2 consumption would then be:

$$-\frac{d[I_2]}{dt} = [I_2][AETSA]\left\{k_4 + \frac{k_6 k_9}{k_9[I^-][H^+] + k_6[AETSA]}\right\} \qquad (II)$$

If one assumes $k_9 \gg k_6$, then a plot of initial rate *vs.* $1/[H^+]$ should give a straight line from which values for k_4 and k_6 can be estimated.

(b) Experimental studies were performed between pH 1 and 2 where complete protonation of the amine part of the amino acid is expected:

$$H_2NCH_2CH_2S{-}SO_3H + H^+ \rightarrow H_3\overset{+}{N}CH_2CH_2S{-}SO_3H \qquad (13a)$$

This was evident from the NMR spectrum of AETSA in acidic medium in which the amine protons could not be observed owing to their rapid exchange with solvent. Thus, when AETSA as a reactant is used in this manuscript, it is referring to the *N*-protonated amino acid. Any further protonation can only occur on the inner sulfur atom. If AETSA forms a pre-equilibrium complex with acid, in which protonation occurs on the inner sulfur atom then it becomes unreactive or less active to electrophilic attack:

$$AETSA + H^+ \rightleftharpoons [AETSA{-}H]^+ \qquad (13b)$$

The rate of reaction then becomes:

$$-\frac{d[I_2]}{dt} = \frac{[I_2][AETSA]_T}{1 + K_{eq}[H^+]}\left\{k_4 + \frac{k_6 k_9}{k_9[I^-][H^+]}\right\} \qquad (III)$$

where $K_{eq} = k_{13}/k_{-13}$ and $[AETSA]_T = [AETSA] + [[AETSA{-}H]^+]$. Eqn. (III) handles both retardations. The $1 + K_{eq}[H^+]$ term in the denominator accounts for the retardation *via* the protonation of AETSA, while the second term accounts for the HOI/I_2 retardation.

Iodate variations

When $[AETSA]_0 \gg [IO_3^-]_0$, the reactions which form oxyiodine species are quickly terminated owing to the depletion of IO_3^-. The little $[I_2]$ formed will be rapidly consumed by the excess AETSA. This explains the progression observed in Fig. 3A(a)–(e). When $[IO_3^-]_0 \approx [AETSA]_0$, the I_2 formed is not rapidly consumed as AETSA would have been depleted by reaction with IO_3^-.

AETSA dependence

When $R \gg 1$, *e.g.* in Fig. 4A(d) ($R = 5$), the [AETSA] is insufficient to produce any transient I_2. Thus, when reaction follows stoichiometry (1), I_2 formed from the subsequent Dushman reaction[21] has insufficient AETSA to consume it, hence the observed monotonic increase of I_2 in Fig. 4A(d). Increase in AETSA produces the reactive species, HOI, I^-, HIO_2 at a much faster rate; hence the shorter induction time.

I_2–AETSA reaction, autoinhibition

Fig. 5A shows how rapidly the I_2–AETSA reaction shuts itself down as the reaction proceeds. This mechanism of self-inhibition involves I_3^-, an inert electrophile. This form of autoinhibition is illustrated in Fig. 6A where addition of I^- effectively halts the reaction. The iodide product from reaction (4) quickly combines with remaining I_2 as in reaction (10), followed by reaction (11).

With the addition of reactions (11) and (9) to reactions (6) and (4), the rate of consumption of I_2 becomes

$$-\frac{d[I_2]}{dt} = [I_2][AETSA]\left\{k_4 + \frac{k_6 k_{-9}}{k_6[AETSA] + k_9[I^-][H^4]} + \frac{k_{10} k_{11}[I^-]}{k_{11}[AETSA] + k_{-10}}\right\} \qquad (IV)$$

If one assumes that both I_3^- and $[AETSA{-}H]^+$ are inert, then eqn. (IV) can be rewritten as:

$$-\frac{d[I_2]}{dt} = \frac{[I_2]_T[AETSA]_T}{(1 + K'_{eq}[I^-])(1 + K_{eq}[H^+])} \times \left\{k_4 + \frac{k_6 k_{-9}}{k_9[I^-][H^+]}\right\} \qquad (V)$$

where $k_6[AETSA]$ was considered negligible and $k_{11} \approx 0$, K'_{eq} is k_{10}/k_{-10} and $[I_2]_T = [I_2] + [I_3^-] + 1/2[I^-]$. Eqn. (V) also takes into account both acid and iodide inhibition in the I_2–AETSA reaction. An analytical solution for eqn. (V) is difficult to obtain. There are always at least two variables at any time. In high acid concentrations where $[H^+]$ is effectively buffered; three variables exist: $[I_2](t)$, $[AETSA](t)$, and $[I^-](t)$. When the reaction is run in high $[I^-]_0$, so as to reduce the number of variables, the reaction effectively shuts down, and no reaction progress is observed (Fig. 6A). From eqn. (III), however, an upper limit for the bimolecular rate constant for the I_2–AETSA reaction, k_4 has been evaluated as 16.7 ± 2.3 M^{-1} s^{-1}. The value of k_4 was calculated from two sets of data: Fig. 5B and Fig. 6B. A plot of initial rate *vs.* $[I^-]_0^{-1}$ gives a straight line of intercept $k_4[I_2][AETSA]_T$. The rate constant for the direct reaction of I_3^- with AETSA, k_{11}, was evaluated as $(5.8 \pm 0.5) \times 10^{-1}$ M^{-1} s^{-1} from the data in Fig. 6B by extrapolation. The value of k_6, reaction of HOI with AETSA, was determined from the set of data in Fig. 7B as 480 ± 5 M^{-1} s^{-1}.

Oxidation of AETSA

Oxidation of AETSA must occur *via* a series of two-electron jumps from the inner sulfur atom. The first step involves the

Table 1 Proposed mechanism for the AETSA–iodate reaction

reaction	rate constant
oxyhalogen reactions	
$IO_3^- + I^- + 2H^+ \rightleftharpoons HIO_2 + HOI$ (M1)	1.44×10^3 M^{-3} s^{-1}, 5×10^{-2} M^{-1} s^{-1}
$HIO_2 + I^- + H^+ \rightleftharpoons 2HOI$ (M2)	2×10^9 M^{-2} s^{-1}, 90 M^{-1} s^{-1}
$HOI + I^- + H^+ \rightleftharpoons I_2 + H_2O$ (M3)	3.1×10^{12} M^{-2} s^{-1}, 2.2 s^{-1}
$IO_3^- + HOI + H^+ \rightleftharpoons 2HIO_2$ (M4)	8.6×10^2 M^{-2} s^{-1}, 2.0 M^{-1} s^{-1}
$I_2 + I^- \rightleftharpoons I_3^-$ (M5)	6.2×10^9 M^{-1} s^{-1}, 8.5×10^7 s^{-1}
oxyhalogen–sulfur reactions	
$H^+ + AETSA \rightleftharpoons [AETSA{-}H]^+$ (M6)	8.5×10^4 M^{-1} s^{-1}, 2.0×10^6 s^{-1}
$HIO_2 + R{-}SSO_3H \rightarrow RS(O)SO_3H + HOI$ (M7)	10 M^{-1} s^{-1}
$HIO_2 + R{-}S(O)SO_3H \rightarrow RS(O_2)SO_3H + HOI$ (M8)	10 M^{-1} s^{-1}
$HOI + R{-}SSO_3H \rightarrow RS(O)SO_3H + I^- + H^+$ (M9)	4.8×10^2 M^{-1} s^{-1}
$HOI + R{-}S(O)SO_3H \rightarrow RS(O_2)SO_3H + I^- + H^+$ (M10)	2.0×10^2 M^{-1} s^{-1}
$HOI + RS(O_2)SO_3H + H_2O \rightarrow RSO_3H + SO_4^{2-} + I^- + 3H^+$ (M11)	75 M^{-1} s^{-1}
$I_2 + RSSO_3H + H_2O \rightarrow RS(O)SO_3H + 2I^- + 2H^+$ (M12)	16.7 M^{-1} s^{-1}
$I_3^- + RSSO_3H + H_2O \rightarrow RS(O)SO_3H + 3I^- + 2H^-$ (M13)	5.8×10^{-1} M^{-1} s^{-1}

The rate constants are written to the right of the equation, with the forward rate constant written first, separated by a comma from the reverse rate constant. The units are also given.

formation of $H_2NCH_2CH_2S(O)SO_3H$ [reactions (4) and (6)]. The bulky nature of AETSA makes dimerizations and any other forms of S—S bond formation unlikely. Most of the AETSA oxidation is carried out by the oxyiodine intermediates HIO_2, HOI and I_2. Further oxidation of $H_2NCH_2CH_2S(O)SO_3H$ will be primarily through HOI. The experiments set up for the stoichiometric determination of the I_2–AETSA reaction prove the importance of HOI in the oxidation of $H_2NCH_2CH_2S(O)_2SO_3H$. Addition of excess base quantitatively converts I_2 to HOI:[31]

$$I_2(aq) + OH^- \rightarrow HOI + I^- \quad (14)$$

Further oxidation then ensues:

$$HOI + H_2NCH_2CH_2S(O)SO_3H \rightarrow H_2NCH_2CH_2S(O_2)SO_3H + H^+ + I^- \quad (15)$$

There is no way of distinguishing mechanistically when the S—S bond is cleaved to yield SO_4^{2-}. The observation that no $BaSO_4$ precipitation is observed at the beginning of the reaction would tend to suggest that the inner S atom is first oxidized to the sulfinic acid (at least) before the S—S bond can be cleaved. Further oxidation of $NH_2CH_2CH_2S(O_2)SO_3H$ will yield:

$$HOI + H_2NCH_2CH_2S(O_2)SO_3H + H_2O \rightarrow H_2NCH_2CH_2SO_3H + SO_4^{2-} + 2H^+ \quad (16)$$

Reaction (16) could be a composite of two steps:

$$H_2NCH_2CH_2S(O_2)SO_3H + H_2O \rightarrow H_2NCH_2CH_2SO_2H + SO_4^{2-} + 2H^+ \quad (17)$$

followed by:

$$HOI + H_2NCH_2CH_2SO_2H \rightarrow H_2NCH_2CH_2SO_3H + I^- + H^+ \quad (18)$$

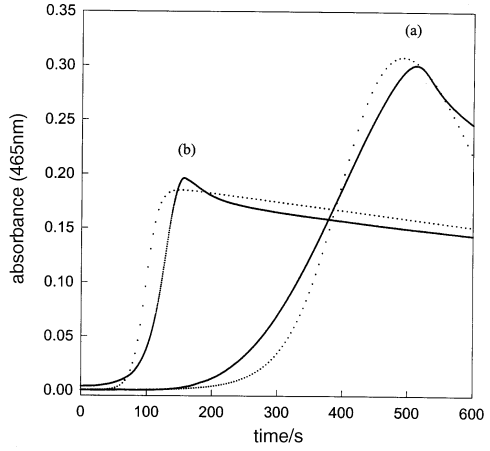

Fig. 9 Comparison of simulations (·····) and experimental (——) for the IO_3^-–AETSA reaction. Traces labelled (a) represent simulations and experimental data at $[H^+]_0 = 0.100$ M, (b) traces are at $[H^+]_0 = 0.800$ M; $[IO_3^-] = 0.001$ M; $[AETSA]_0 = 0.005$ M.

Computer simulations

Our experimental observations simplified our proposed mechanism by eliminating some possible reactions which could be determined as being ineffective. A good example is the oxidation of $H_2NCH_2CH_2S(O)SO_3H$ by I_2 which has not been used in the chemical reaction network. The reaction network has 13 reactions which were easily divided into two sets: the oxyiodine reactions and the oxyiodine–AETSA reactions. These reactions are presented in Table 1 [reactions (M1)–(M13)]. The first five reactions are the standard oxyiodine reactions whose kinetics parameters are well known. The kinetics parameters for reactions (M1)–(M4) were taken from the work of Furrow and Noyes[32] and Treindl and Noyes.[33] The kinetics parameters for reaction (M5) were taken from a Raman laser temperature-jump study of Ruasse *et al.*[34] I^- is a reactant in four of these five reactions as the control species [reaction (M2)] and as the autoinhibitory reagent [reaction (M5)].

The oxyiodine–sulfur reactions involve the oxidation of a sulfur centre coupled with the reduction of an iodine centre. No attempt was made to produce and use the exact rate parameters for the protolytic reaction (M6). These parameters could be varied over wide ranges with very small changes in overall global dynamics of the reaction system. The use of higher (and more realistic) kinetics parameters for the protolytic reaction increased the complexity of the integration, thus requiring long periods of time for calculations to be completed. Oxidation reactions by HIO_2 [reactions (M7) and (M8)] have been included in this network even though they will not be very effective as the reaction proceeds. Reaction (M8), especially, will be useful at the beginning of the reaction.

After production of I^-, however, HOI will carry most of the oxidation through the rapid equilibrium reaction (M2). Reactions (M9), (M10) and (M11) show the step-wise oxidation of AETSA to the sulfonic acid and sulfate. For these simulations it was assumed that the cleavage of the S—S bond occurs together with a two-electron oxidation of the inner sulfur atom. Reactions (M12) and (M13) show the oxidation of AETSA by the molecular iodine species. The rate constant, k_{11}, for the oxidation of AETSA by I_3^- was evaluated by this study and was low enough to account for the autoinhibition. All the oxyiodine–AETSA reactions were taken as irreversible.

The 13 rate equations in Table 1 were numerically integrated using a semi-implicit Runge Kutta method.[35] There was good agreement between the experimental data and the computer simulations. The mechanism was tested for the effects of acid, iodide and iodate. Fig. 9 shows the fit to the data for the effect of acid. The slight deviations obtained were as a result of the other species which have slight absorptivities at 465 nm. Our simulations follow strictly the concentrations of I_2 only.

Conclusion

Our proposed mechanism is the most concise that can be generated and yet still fully explain the observed reaction dynamics. An important subset of reactions completely ignored in this mechanism is the group of sulfur–sulfur reactions. These can help, especially, to explain what happens to the intermediate sulfur species in excess reductant. Through autooxidations and disproportionations, the sulfur centres will eventually end up in the preferred oxidation states of -2, 0 and $+6$. By maintaining HOI as the sole important oxidant in solution, errors that might arise from omitting sulfur–sulfur reactions have been minimized. For example, two sulfinic acid centres can disproportionate:

$$S^{II} + S^{II} \rightarrow S^{IV} + S^{O} \quad (19)$$

There is no quantitative way of measuring sulfate production as the reaction proceeds, although experimental data shows that sulfate production is not immediate (there is a time lag between mixing of solution and production of $BaSO_4$ precipitate). If sulfate production can be properly monitored, then it will be easier to predict the point of S—S bond cleavage.

The NMR data strongly suggest that the initial step is the formation of the sulfone and not the cleavage of the S—S bond. Cleavage of the S—S bond, it appears, occurs effectively when each of the sulfur atoms is coordinately saturated.

We would like to acknowledge helpful discussions with Professors Jonnalagadda and Martincigh. This work was supported by a grant from the National Science Foundation (Grant Number CHE—9632592).

References

1 C. R. Chinake and R. H. Simoyi, *J. Phys. Chem.*, 1996, **100**, 1643.
2 E. Mambo and R. H. Simoyi, *J. Phys. Chem.*, 1993, **97**, 13662.
3 C. R. Chinake, E. Mambo and R. H. Simoyi, *J. Phys. Chem.*, 1994, **95**, 2908.
4 J. B. Jones, C. R. Chinake and R. H. Simoyi, *J. Phys. Chem.*, 1995, **99**, 1523.
5 S. Hashimoto and J. Sunamoto, *Bull. Chem. Soc. Jpn.*, 1966, **39**, 1207.
6 Y. Luo, M. Orban, K. Kustin and I. R. Epstein, *J. Am. Chem. Soc.*, 1989, **111**, 4541.
7 I. R. Wilson and G. M. Harris, *J. Am. Chem. Soc.*, 1960, **82**, 4515.
8 I. R. Wilson and G. M. Harris, *J. Am. Chem. Soc.*, 1961, **84**, 1101.
9 M. R. Hoffman, *Environ. Eng. Sci.*, 1977, **11**, 61.
10 R. J. Field, E. Koros and R. M. Noyes, *J. Am. Chem. Soc.*, 1972, **94**, 8649.
11 R. M. Noyes, *Ber. Bunsen-Ges. Phys. Chem.*, 1980, **84**, 295.
12 B. P. Belousov, *Sb. Ref. Radiat. Med.*, 1959, **145**, 1958.
13 A. M. Zhabotinsky, *Dokl. Akad. Nauk SSSR.*, 1959, **157**, 392.
14 W. C. Bray, *J. Am. Chem. Soc.*, 1921, **43**, 1262.
15 G. Nicolis and J. Portnow, *Chem. Rev.*, 1973, **73**, 371.
16 T. C. Briggs and W. C. Rauscher, *J. Chem. Educ.*, 1973, **50**, 496.
17 R. M. Noyes, *J. Am. Chem. Soc.*, 1980, **102**, 4644.
18 R. J. Field and R. M. Noyes, *J. Chem. Phys.*, 1974, **60**, 1877.
19 D. Banard, *J. Chem. Soc.*, 1957, 4675.
20 G. Rabai and M. Beck, *J. Chem. Soc., Dalton Trans.*, 1985, 1669.
21 S. J. Dushman, *J. Phys. Chem.*, 1904, **8**, 453.
22 A. D. Autrey and R. E. Connick, *J. Am. Chem. Soc.*, 1953, **73**, 1842.
23 D. A. Skoog and D. M. West, *Analytical Chemistry: An Introduction*, Saunders College Publishing, San Francisco 4th edn., 1986, p. 83.
24 H. Landolt, *Ber. Dtsch. Chem. Ges.*, 1886, **19**, 1313.
25 D. C. Harris, *Quantitative Chemical Analysis*, W. H. Freeman and Co., San Francisco, 1982, p. 384.
26 P. Soupart, in *Amino Acid Pools*, ed. J. T. Holden, Elsevier, New York, 1962, pp. 220–262.
27 J. G. Jacobson and L. H. Smith, *Physiol. Rev.*, 1968, **48**, 424.
28 In the oxidation of thiourea by Br_2(aq), for example, an increase in the reductant concentration (thiourea) increased the induction period, see R. H. Simoyi and I. R. Epstein, *J. Phys. Chem.*, 1987, **91**, 5124.
29 R. M. Noyes, L. V. Kalachev and R. J. Field, *J. Phys. Chem.*, 1995, **99**, 3514.
30 M. Eigen and K. Kustin, *J. Am. Chem. Soc.*, 1962, **84**, 1355.
31 T. R. Thomas and D. T. Pence, *J. Inorg. Nucl. Chem.*, 1980, **42**, 183.
32 S. D. Furrow and R. M. Noyes, *J. Am. Chem. Soc.*, 1982, **104**, 38.
33 L. Treindl and R. M. Noyes, *J. Phys. Chem.*, 1993, **97**, 11354.
34 M-F. Ruasse, J. Aubard, B. Galland and A. Adenier, *J. Chem. Phys.*, 1986, **90**, 4382.
35 P. Kaps and P. Rentrop, *Numer. Math.*, 1979, **23**, 55.

Paper 6/06729H; *Received* 1st *October*, 1996